Cloaking the underlying long-range order of randomly perturbed lattices

Michael A. Klatt [1,*] Jaeuk Kim,[1,†] and Salvatore Torquato[1,2,‡]

[1]*Department of Physics, Princeton University, Princeton, New Jersey 08544, USA*
[2]*Department of Chemistry, Princeton Institute for the Science and Technology of Materials, and Program in Applied and Computational Mathematics, Princeton University, Princeton, New Jersey 08544, USA*

Random, uncorrelated displacements of particles on a lattice preserve the hyperuniformity of the original lattice, that is, normalized density fluctuations vanish in the limit of infinite wavelengths. In addition to a diffuse contribution, the scattering intensity from the the resulting point pattern typically inherits the Bragg peaks (long-range order) of the original lattice. Here we demonstrate how these Bragg peaks can be hidden in the effective diffraction pattern of independent and identically distributed perturbations. All Bragg peaks vanish if and only if the sum of all probability densities of the positions of the shifted lattice points is a constant at all positions. The underlying long-range order is then "cloaked" in the sense that it cannot be reconstructed from the pair correlation function alone. On the one hand, density fluctuations increase monotonically with the strength of perturbations a, as measured by the hyperuniformity order metric $\overline{\Lambda}$. On the other hand, the disappearance and reemergence of long-range order, depending on whether the system is cloaked as the perturbation strength increases, is manifestly captured by the τ order metric. Therefore, while the perturbation strength a may seem to be a natural choice for an order metric of perturbed lattices, the τ order metric is a superior choice. It is noteworthy that cloaked perturbed lattices allow one to easily simulate very large samples (with at least 10^6 particles) of disordered hyperuniform point patterns without Bragg peaks.

I. INTRODUCTION

A common way to introduce disorder into an otherwise ordered system, such as a perfect crystal or quasicrystal, is to randomly perturb the particle positions of that system [1–4]. A *perturbed lattice* is a point pattern (process) in d-dimensional Euclidean space $\mathbb{R}^d$ obtained by displacing each point in a Bravais lattice [5] according to some stochastic rule [1,6–8]. Perturbed lattices have been intensively studied in a broad range of contexts, from statistical physics and cosmology [9,10], to crystallography [1,2], or to probability theory, including distributions of zeros of random entire functions [11] and number rigidity [12–14]. They are related to certain queueing problems [15], in particular, G processes [16], and stable matchings in any dimension [14]. Perturbed lattices are moreover used to generate disordered initial configurations for numerical simulations [17] or configurations of sampling points [18].

The simplest stochastic rule involves independent and identically distributed perturbations. This model is also known as a *shuffled lattice* [9,19]. The choice of the distribution of perturbations then specifies the model. A typical stochastic rule is the Gaussian distribution [12], in which case the model is also called an *Einstein pattern* [20]. Alternatively, the distributions can have heavy tails like the Cauchy or the Pareto distributions [8].

Another stochastic rule of special interest in the present study is where each point in a Bravais lattice $\mathcal{L}$ [21] is displaced by a random vector that is uniformly distributed on a rescaled unit cell $aC := \{\boldsymbol{x} \in \mathbb{R}^d : \boldsymbol{x}/a \in C\}$, where $a > 0$ is a scalar factor and C is a unit cell of the lattice. We henceforth refer to this case as the *uniformly randomized lattice* (URL) model. We will use it as the main example for our more general results on the "cloaking" of Bragg peaks. The constant a controls the strength of perturbations. Counterintuitively, the long-range order in two-point statistics suddenly disappears at certain discrete values of a and reemerges for stronger perturbations, as we will show.

For simplicity, we here use the simple cubic lattice $\mathcal{L} = \mathbb{Z}^d$ with $aC := [-a/2, a/2]^d$, see Fig. 1. It is a popular model studied in the optics community, among others, where it is used to understand how the introduction of disorder in lattices
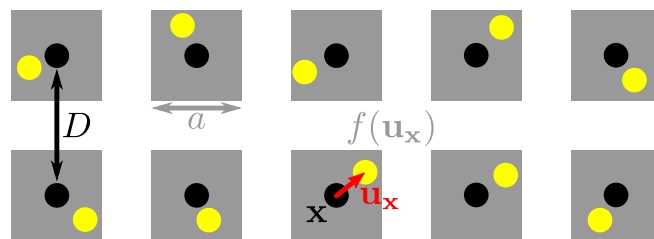

FIG. 1. The uniformly randomized lattice (URL) model: Each lattice point $\boldsymbol{x}$ in $\mathbb{Z}^d$ is shifted by a random displacement $\boldsymbol{u_x}$. The latter is uniformly distributed on $[-a/2, a/2]^d$. In general, D denotes a characteristic length scale of the system. Here it is the lattice constant $D = 1$.

*mklatt@princeton.edu
†jaeukk@princeton.edu
‡torquato@princeton.edu

032118-1

influences the resultant optical properties of the materials [3,4,22–30].

Perturbed lattices are special cases of hyperuniform systems. A hyperuniform point pattern is one in which the structure factor $S(\boldsymbol{k}) := 1 + \rho \tilde{h}(\boldsymbol{k})$ tends to zero as the wave number $k := \|\boldsymbol{k}\|$ tends to zero [19,31]:

$$\lim_{\|\boldsymbol{k}\| \to 0} S(\boldsymbol{k}) = 0, \tag{1}$$

where $\tilde{h}(\boldsymbol{k})$ is the Fourier transform of the total correlation function $h(\boldsymbol{r}) = g_2(\boldsymbol{r}) - 1$ and $g_2(\boldsymbol{r})$ is the standard pair correlation function. This implies that infinite-wavelength density fluctuations are anomalously suppressed.

An equivalent definition of hyperuniformity is based on the local number variance $\sigma^2(R)$, which is associated with the number $N(R)$ of points within a spherical observation window B_R of radius R. A point pattern in $\mathbb{R}^d$ is hyperuniform if its local number variance $\sigma^2(R) := \mathbb{V}ar[N(R)]$ grows in the large-R limit slower than R^d. This is in contrast to typical disordered systems, such as Poisson point patterns and liquids where the number variance scales like the volume $v_1(R)$ of the observation window, for example, see Ref. [31].

If the structure factor vanishes at the origin continuously, then its asymptotic behavior

$$S(\boldsymbol{k}) \sim |\boldsymbol{k}|^\alpha \quad \text{for } |\boldsymbol{k}| \to 0 \tag{2}$$

with $\alpha > 0$ determines the large-R asymptotic scaling of the number variance [19] for $R \to \infty$:

$$\sigma^2(R) \sim \begin{cases} R^{d-1}, & \alpha > 1 \text{ (class I)} \\ R^{d-1} \ln R, & \alpha = 1 \text{ (class II)} \\ R^{d-\alpha}, & \alpha < 1 \text{ (class III)} \end{cases} . \tag{3}$$

These scalings of $\sigma^2(R)$ define three classes of hyperuniformity [31], with class I and III describing the strongest and weakest forms of hyperuniformity, respectively.

Perturbed lattices with independent and identically distributed displacements are always hyperuniform, but the hyperuniformity class depends on whether the first and second moments of the perturbations exist [6,8]. If both exist, then the perturbed lattice is class I hyperuniform with $\sigma^2(R) \sim R^{d-1}$, that is, the number variance grows like the surface area of the observation window. Further examples of class I hyperuniform systems are all crystals [19], many quasicrystals [32], certain random organization models [33], certain nonequilibrium dynamic states with active particles [34], some stable matchings [14], one-component plasmas [35,36], the Ginibre process related to random matrices [36–38], and hyperuniform disordered ground states [39,40]. The latter have been found particularly useful for optical applications, including photonic band-gap materials [41], light extraction [42,43], and transparent low-density amorphous materials [44]. Examples of class II hyperuniform systems include some quasicrystals [32], the ground state of superfluid helium [45,31], ground states of free spin-polarized fermions [46], maximally random jammed particle packings [47,48], and perfect glasses [40]. Examples of class III hyperuniform systems include certain classical disordered ground states [49], random organization models [50], and perfect glasses [40].

In hyperuniform systems, the suppression of large-scale density fluctuations can be quantitatively characterized by the *hyperuniformity order metric* [19,31]. For class I systems, it is defined as

$$\overline{\Lambda} := \lim_{L \to \infty} \frac{1}{L} \int_0^L \frac{\sigma^2(R)}{(R/D)^{d-1}} dR, \tag{4}$$

where D is a characteristic length scale in the system, e.g., the lattice constant.

A different measure of order in general statistically homogeneous point patterns is the τ order metric [39]. It measures deviations of two-point statistics (i.e., structure factor and pair correlation function) from that of the ideal gas (Poisson point process):

$$\tau := \frac{1}{D^d} \int_{\mathbb{R}^d} [g_2(\boldsymbol{r}) - 1]^2 d\boldsymbol{r}$$

$$= \frac{1}{(2\pi)^d D^d \rho^2} \int_{\mathbb{R}^d} [S(\boldsymbol{k}) - 1]^2 d\boldsymbol{k}. \tag{5}$$

By definition, $\tau = 0$ for the homogeneous Poisson point process with $g_2(\boldsymbol{r}) = S(\boldsymbol{k}) = 1$. By contrast, $\tau = \infty$ if there is a Bragg peak contribution to $S(\boldsymbol{k})$ (because of the squared difference).

In what follows, we will compute both $\overline{\Lambda}$ and τ to thoroughly characterize the degree of order and disorder in hyperuniform perturbed lattices. Currently, perturbed lattices with weak or no correlations are among the rare examples of amorphous hyperuniform point patterns that can be easily simulated with a million particles per sample [8,14,51,52]. However, in general, the resulting point patterns are not fully amorphous in the sense that their structure factor exhibits Bragg peaks, which are "inherited" from the original lattice.

We demonstrate how a fine-tuned distribution of perturbations can hide or "cloak" all or a portion of these Bragg peaks. The cloaking of Bragg peaks obscures the underlying long-range order in the sense that it cannot be reconstructed from two-point statistics alone [53]. This phenomenon has been largely unnoticed in the community [54].

Here we provide an explicit real-space condition, present and discuss examples, and comprehensively structurally characterize the URL models using two different order metrics. First, we provide an intuitive necessary and sufficient criterion in Sec. II and discuss examples in Sec. III. We also prove that perturbed lattices with independent and identically distributed displacements cannot be stealthy, which would require that $S(\boldsymbol{k}) = 0$ for all $\boldsymbol{k}$ in a neighborhood around the origin. In Sec. IV, we show that while the density fluctuations measured by $\overline{\Lambda}$ increase for stronger perturbations, the degree of order measured by τ reveals a dramatic difference between the cloaked cases (no long-range order) and uncloaked cases (long-range order). While for the former τ is finite, it diverges for the latter. In that case, the rate by which τ increases with the system size still characterizes the degree of order in the system [55]. An outlook on related and open problems is given in the concluding Sec. V.

II. NECESSARY AND SUFFICIENT CONDITION FOR CLOAKING

We here consider uncorrelated displacements $\boldsymbol{u_x}$ that follow the same probability density function $f(\boldsymbol{u_x})$ for each point
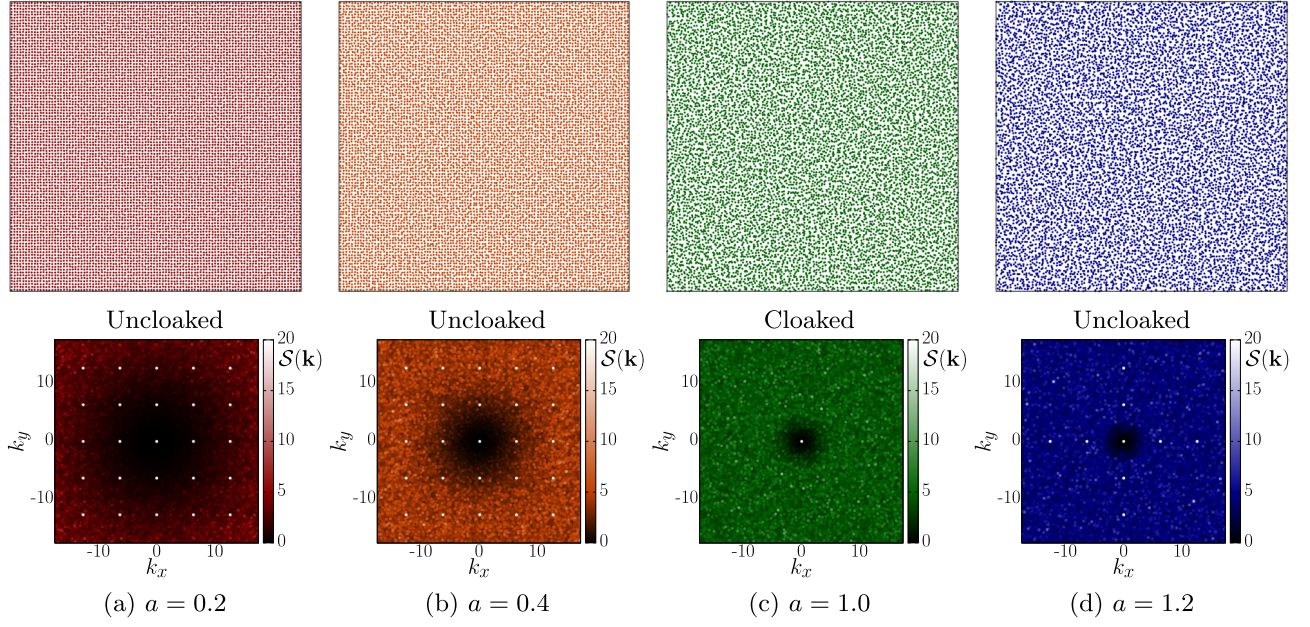
FIG. 2. Structure factors of URL models in two dimensions, where the perturbation strength a increases from left to right. Samples of point patterns are shown on top, structure factors $\mathcal{S}(\boldsymbol{k})$ of single configurations (including the forward scattering) are shown below, represented by the color code (gray scale values), as a function of the two-dimensional wave vector $\boldsymbol{k} := (k_x, k_y)$. The Bragg peaks vanish when the perturbations cover the entire space without overlap ($a = 1.0$) but reappear when the perturbations become stronger ($a = 1.2$). In the last case, only peaks with $k_x = 0$ or $k_y = 0$ are clearly visible, while other peaks have small weights.

$\boldsymbol{x}$ in a lattice $\mathcal{L}$, see Fig. 1. The structure factor $S(\boldsymbol{k})$ is then given by [6]:

$$S(\boldsymbol{k}) = 1 - |\tilde{f}(\boldsymbol{k})|^2 + |\tilde{f}(\boldsymbol{k})|^2 \, S_{\mathcal{L}}(\boldsymbol{k}) \,, \qquad (6)$$

where $S_{\mathcal{L}}(\boldsymbol{k})$ is the structure factor of the unperturbed lattice $\mathcal{L}$ and $\tilde{f}$ is the characteristic function of the perturbations, that is, the Fourier transform of f. For convenience, the formula, which holds for more general point patterns, is rederived in Appendix A.

Since the characteristic function is uniformly continuous at the origin, and since $\tilde{f}(\boldsymbol{0}) = 1$, the perturbed point pattern is hyperuniform if and only if the original point pattern is hyperuniform. Hyperuniformity is preserved even if the moments of the perturbations do not exist, but in that case the class of hyperuniformity changes (that is, the asymptotic behavior of the structure factor at the origin) [8,31].

If the second moment of the random displacement diverges, but the first moment remains finite (like for a Cauchy distribution), then the perturbed lattice changes from a class I hyperuniform system to a class II hyperuniform system [6,8]. If also the first moment diverges (like for a Pareto distribution), then the perturbed lattice becomes a class III hyperuniform system [6,8].

In class I, the strongest possible hyperuniform scaling of uncorrelated perturbed lattices is k^2 [6,8]. Stealthy hyperuniformity can never be preserved by independent random perturbations, as we prove in Appendix B.

Equation (6) shows that a perturbed lattice will generally exhibit the same Bragg peaks as the original lattice. We can, however, choose the distribution of perturbations such that the characteristic function $\tilde{f}$ vanishes at these positions [6,54]. Intuitively speaking, the effective diffraction pattern of the perturbations cloaks the Bragg peaks.

The pair correlation function offers an equivalent, intuitive criterion for the vanishing of all Bragg peaks. To obtain a statistically homogeneous point pattern, called *stationarized lattice*, we simultaneously shift all lattice points by a random vector that is uniformly distributed within a primitive unit cell of the lattice. The pair correlation function of the perturbed lattice is then given by:

$$g_2(\boldsymbol{r}) = \frac{1}{\rho} f * \sum_{\boldsymbol{x} \in \mathcal{L}} f(\boldsymbol{r} - \boldsymbol{x}) - \frac{1}{\rho} f * f(\boldsymbol{r}), \qquad (7)$$

where ρ is the number density and $*$ denotes the convolution operator. The proof is given in Appendix C.

All Bragg peaks vanish if and only if the series in Eq. (7) is constant, that is, independent of position $\boldsymbol{r}$:

$$\sum_{\boldsymbol{x} \in \mathcal{L}} f(\boldsymbol{r} - \boldsymbol{x}) = \rho, \qquad (8)$$

which means that the sum of the probability density functions for all shifted lattices points add up to a constant function. By normalization, this constant has to be the number density. If this condition (8) is met, then the resulting cloaked perturbed lattices have the following structure factor and pair correlation function, respectively:

$$S(\boldsymbol{k}) = 1 - |\tilde{f}(\boldsymbol{k})|^2 \quad \text{and} \quad g_2(\boldsymbol{r}) = 1 - \frac{1}{\rho} f * f(\boldsymbol{r}).$$

III. EXAMPLES OF CLOAKED AND UNCLOAKED PERTURBED LATTICES

A straightforward example how a lattice can be cloaked by perturbations is the uniform distribution of each lattice point within its unit cell. Our simulation study, shown in Fig. 2,
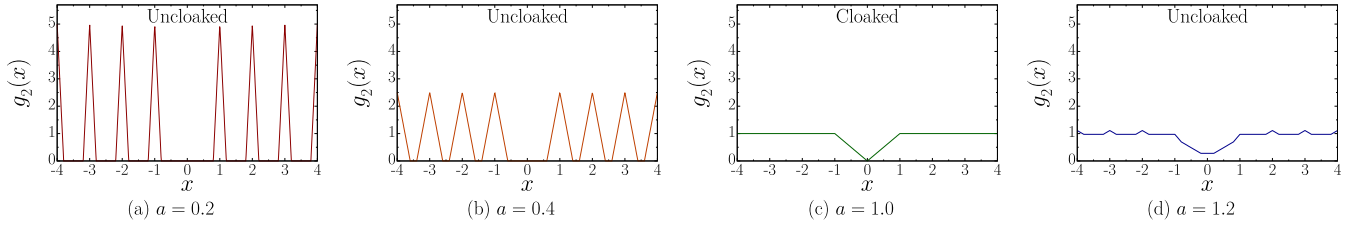
FIG. 3. Pair correlation functions $g_2(x)$ of the URL model in one dimension, cf. Eqs. (7) and (C6), where the random displacement of each point in the lattice $\mathbb{Z}$ is uniformly distributed in $[-a/2, a/2)$. For $a = 1.0$, the pair correlation function lacks any periodicity, see Eq. (C7), and hence, the Bragg peaks are cloaked; for the angular-averaged pair correlation function in the first three dimensions, see Fig. 5.

demonstrates the appearance and cloaking of Bragg peaks for URL models in two dimensions (2D), see Fig. 1.

We simulate four samples for different values a, each containing 10 000 points subject to periodic boundary conditions. Figure 2 shows the resulting point patterns in the upper panels and 2D plots of their structure factor [56] in the lower panels. If the perturbation strength a is an integer multiple of the lattice constant D, then Eq. (8) is fulfilled and the Bragg peaks are cloaked.

Figure 3 shows the pair correlation functions for the same parameters but in 1D for better visualization. Only in the cloaked models with $a \in \mathbb{N} \setminus \{0\}$, $g_2(x)$ is not periodic for $\|x\| > a$. For the 1D model with $a = 1$, $g_2(x)$ was previously derived by Torquato and Stillinger [19].

We see that increasing the strength of the perturbations does generally not lead to a monotonic decay of the weights of Bragg peaks. Instead, these weights oscillate as shown in Fig. 4. So, interestingly, Bragg peaks can vanish for specific distributions of the random shifts, but they reappear as the perturbations become stronger. Fine-tuned perturbations at which the system appears to be without long-range order according to the two-point functions allow for the simulation of million-particle samples of hyperuniform systems without Bragg peaks. For these cloaked URLs, Fig. 5 shows for 1D, 2D, and 3D, the angular average of the structure factor $S(k)$ as a function of the wave number k and the angular average of

the pair correlation function $g_2(r)$ as a function of the radial distance.

One could ask to what extent is the underlying long-range order cloaked with respect to the higher-order functions? Interestingly, for a cloaked URL with $a = 1$, we can actually express all of the n-point correlation functions explicitly by certain intersection volumes. Toward this end, we define $C_{ij} := (C + \boldsymbol{x}_i) \cap (C + \boldsymbol{x}_j)$ and $C^*_{ij} := C \cap \bigcup_{\boldsymbol{x} \in \mathcal{L}} (C_{ij} + \boldsymbol{x})$, where $C + \boldsymbol{x}$ denotes the translation of C by $\boldsymbol{x}$. Then, in case of a statistically homogeneous model (using a stationarized lattice), the multipoint correlation function is given by

$$g_n(\boldsymbol{x}_1, \ldots \boldsymbol{x}_n) = 1 - \frac{1}{|C|} \left| \bigcup_{\substack{i,j=1,\ldots n \\ i \neq j}} C^*_{ij} \right|, \quad (9)$$

where here $|\cdot|$ denotes the volume of a set and C is a unit cell of the lattice $\mathcal{L}$. For a proof, see Appendix D. There, we also show plots of the three-point and four-point correlation functions for the 1D case. While g_3 does not exhibit explicit features of the underlying long-range order, there are specific paths in the parameter space of g_4 that reveal the periodicity of the original lattice.

A less-obvious example of cloaked Bragg peaks is derived from independent and identically distributed perturbations with a probability density function $f(x) = [2 \sin^2(x/2)]/(\pi x^2)$. Due to its heavy tail, its characteristic function has bounded support: $\tilde{f}(k) = (1 - |k|)\mathbf{1}_{[0,1]}(|k|)$, where $\mathbf{1}_A(x)$ is the indicator function of a set A. The resulting structure factor is not analytic at the origin: $S(k) \sim k$ for $k \to 0$. The model is class II hyperuniform [31].

IV. DENSITY FLUCTUATIONS AND ORDER METRICS

Next we focus on class I hyperuniform perturbed lattices, that is, for perturbations with finite first and second moments. In particular, we study the URL with $\mathcal{L} = \mathbb{Z}^d$. To quantify density fluctuations and the degree of order in the system we compute both the hyperuniformity order metric $\overline{\Lambda}$ and the τ order metric.
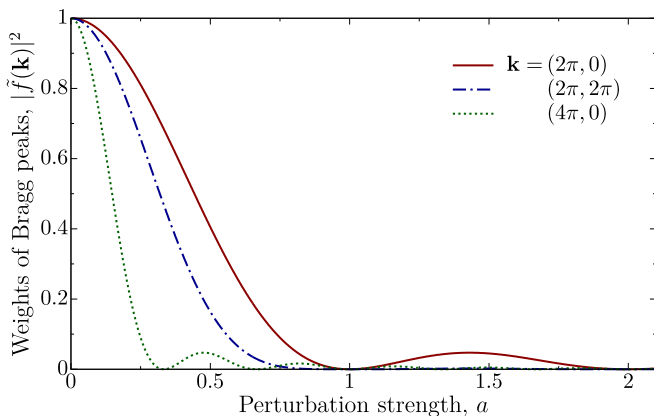

FIG. 4. The weights of the first three Bragg peaks of the 2D URL (cf. Fig. 2) as a function of the perturbation strength a. The three curves correspond to the values of $|\tilde{f}(\mathbf{k})|^2$ at three different peak positions (wave vectors) as indicated in the legend.

A. Hyperuniformity order metric $\overline{\Lambda}$

The local number variance $\sigma^2(R)$ can be expressed in terms of a weighted integral over the structure factor [19]:

$$\sigma^2(R) = \frac{\rho v_1(R)}{(2\pi)^d} \int_{\mathbb{R}^d} S(\boldsymbol{k}) \tilde{\alpha}_2(k; R) d\boldsymbol{k} \quad (10)$$
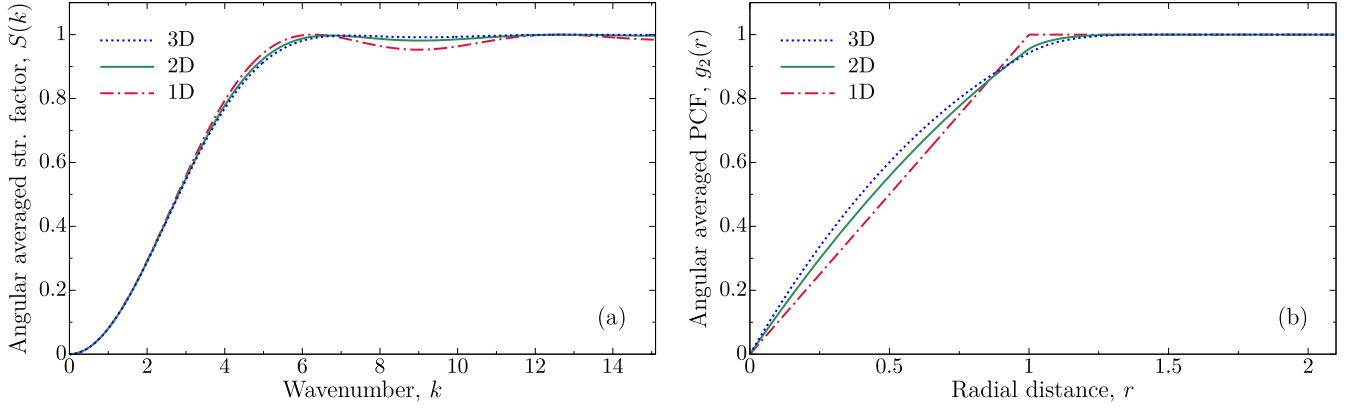
FIG. 5. Angular average of (a) the structure factor $S(k)$ and (b) the pair correlation function $g_2(r)$ for the cloaked URL with $a = 1$ in the first three dimensions. It is apparent that there are no Bragg peaks in $S(k)$ and that $g_2(r)$ lacks any periodicity.

with $\tilde{\alpha}_2(k; R) := 2^d \pi^{d/2} \Gamma(1 + d/2)[J_{d/2}(kR)]^2/k^d$, which is the square of the Fourier transform of the indicator function of B_R divided by $v_1(R)$, $J_\nu(x)$ is the Bessel function of the first kind of order ν.

We compute the hyperuniformity order metric $\overline{\Lambda}$ of class I hyperuniform systems by substituting Eq. (6) into Eqs. (10) and (4). Using $\lim_{L\to\infty} \frac{1}{L} \int_0^L \tilde{\alpha}_2(q; R) R dR = (2\pi)^d/[\pi v_1(1)|q|^{d+1}]$, we obtain:

$$\overline{\Lambda} = \frac{(2\pi D)^d \rho}{\pi D} \left[\int_{\mathbb{R}^d} \frac{1 - |\tilde{f}(k)|^2}{(2\pi)^d |k|^{d+1}} dk + \rho \sum_{q \in \mathcal{L}^* \setminus \{0\}} \frac{|\tilde{f}(q)|^2}{|q|^{d+1}} \right],$$
(11)

where $\mathcal{L}^*$ is the reciprocal lattice of $\mathcal{L}$. The first term originates from the continuous contribution to $S(k)$ in Eq. (6) and the second term from the Bragg peak contribution. Both terms are non-negative. If $f(r)$ is a uniform distribution on a compact domain K and if the domains of different lattice points do not overlap, then the second term equals the hyperuniformity order metric of a crystal, where each site in $\mathcal{L}$ is decorated with K.

For the URL, $\overline{\Lambda}$ is a function of the perturbation strength a. In 1D for $\mathcal{L} = \mathbb{Z}$, we obtain the explicit expression

$$\overline{\Lambda}(a) = \frac{a}{3} + \frac{\mathrm{frac}(a)^2 [1 - \mathrm{frac}(a)]^2}{6a^2},$$
(12)

where $\mathrm{frac}(a)$ denotes the fractional part of a. For $a = 1$, $\overline{\Lambda} = 1/3$ was first derived by Torquato and Stillinger [19]. While the second term in Eq. (12), that is, the Bragg contribution, vanishes for large values of a, the first term grows linearly with a. This behavior holds in any dimension in the sense that

$$\overline{\Lambda}(a) = ca + \mathcal{O}(a^{-2d}), \quad \text{for } a \to \infty,$$
(13)

where c is a constant independent of a [57] and $\mathcal{O}(a^{-2d})$ represents a vanishing bound on the Bragg contribution in Eq. (11) [58].

Figure 6 shows explicit values for 2D obtained from Eq. (11) by numerical integration and by truncating the series at $|q| < 2\pi \times 5000$. Table I lists some of the values from Fig. 6.

The hyperuniformity order metric $\overline{\Lambda}$ is a monotonically increasing function of the perturbation strength a. Stronger perturbations imply strong density fluctuations.

B. The τ order metric

There is, however, a dramatic difference in the degree of order as quantified by the τ order metric [39], see Eq. (5) and Table I. At the two-point level, the τ order metric captures a structural transition between cloaked and uncloaked URLs.

The concept of τ can be used to distinguish the degree of order in perturbed lattices even in the presence of Bragg peaks. To that end, $\tau(L)$ has been defined as a function of system size [55,59]:

$$\tau(L) := \frac{1}{D^d} \int_{[-L,L]^d} [g_2(r) - 1]^2 dr,$$
(14)

so that its growth rate can be considered in the large-L limit. A linear growth in the order metric was first identified in the integer lattice, prime numbers, and limit-periodic systems [55].

Figure 7 shows $\tau(L)$ for a 2D URL. For all noninteger values of a, $\tau(L)$ detects the long-range order and diverges for $L \to \infty$. The steplike periodic variations in the increase of the τ order metric result from the periodicity of the pair correlation function. While for small values of L, the degree of order
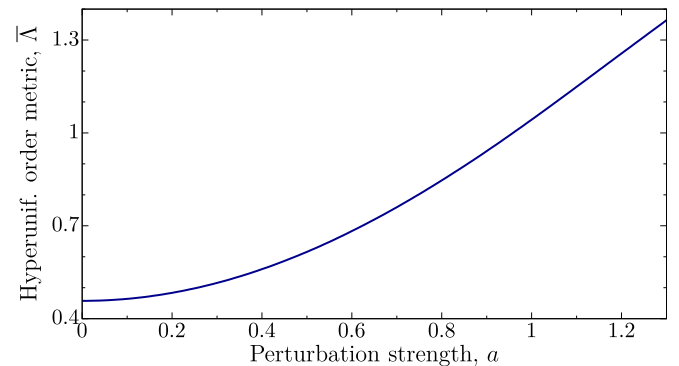

FIG. 6. The hyperuniformity order metric $\overline{\Lambda}$ of the 2D URL as a function of the perturbation strength a. Stronger perturbations imply stronger density fluctuations.

TABLE I. For the 2D URL, we report both the hyperuniformity order metric $\overline{\Lambda}$, which quantifies large-scale density fluctuations, and the τ order metric integrated over the entire system, which quantifies deviations from the ideal gas. If $\tau(\infty) = \infty$, then systems can still be distinguished by the growth rate of τ. The values for the unperturbed lattice are in agreement with those in Ref. [19].

	$\mathbb{Z}^2$	Perturbed lattices				Ideal gas
a	0	1/2	1	3/2	10	∞
$\overline{\Lambda}$	0.4576	0.63148	1.0428	1.5735	10.428	∞
$\tau(\infty)$	∞	∞	2/3	∞	2/30	0

seems to decrease monotonically with increasing perturbation strength a, the curves of $\tau(L)$ cross at intermediate values of L. This nontrivial degree of long-range order as a function of a can be quantified by the growth rate of $\tau(L)$. This growth rate vanishes for $a \to \infty$, but it does not decrease monotonically. Instead, it oscillates as a function of a, vanishes for integer values of a, and reemerges in between. In that sense, a does unexpectedly not directly quantify the degree of order in a URL.

If $a \in \mathbb{N}$ (excluding zero), then the Bragg peaks are cloaked, in which case the order metric converges to a constant:

$$\tau(L) = \left(\frac{2}{3a}\right)^d, \quad \text{for } L \geqslant a.$$

This constant decreases monotonically with increasing integer values of a.

V. CONCLUSIONS AND OUTLOOK

Often for general perturbed lattices, pair statistics are sufficient to detect the underlying long-range order via Bragg peaks. However, the latter are hidden by independent and identically distributed perturbations if and only if the char-
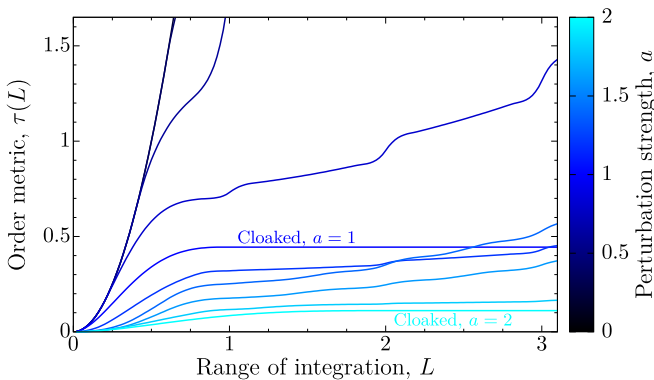

FIG. 7. The τ order metric as a function of system size L of a 2D URL. For almost all values of a, $\tau(L)$ diverges. Since the growth rate is small for $a > 1$, there is a range of values of L where $\tau(L)$ is larger for $a = 1$ (cloaking) than, e.g., at $a = 1.4$ (noncloaking). However, the curves cross at intermediate values of L. While $\tau(L)$ has converged to a constant at $L = 1$ for $a = 1$, it diverges for $a = 1.4$.

acteristic function of the perturbations vanishes at the wave vectors of all reciprocal lattice points.

An equivalent real-space condition is that the probability density functions of the positions of all perturbed lattice points add up to a constant, see Eq. (8). This condition can be easily met for any Bravais lattice by uniformly distributing the lattice points inside their unit cells, that is, for any URL model with $a = 1$. In fact, this holds for any integer value of $a > 0$.

Specifically for the URL, the perturbation strength a at first glance may seem to be a natural metric of order in the system. Counterintuitively, we have shown in the present work that although the degree of long-range order is damped for large perturbations, it oscillates as a function of a. Long-range correlations in two-point statistics can vanish at specific values of a and reemerge for stronger perturbations; see Fig. 2. Our investigation has revealed that the τ order metric is a superior descriptor to quantify both short- and long-range order in the system.

Interestingly, the 1D perturbed lattice with uniform perturbations in the unit cell can be seen as a "two-point dual" of a Fermi-sphere point process [46], which means that the functional form of the structure factor of the former coincides with the pair correlation function of the latter and vice versa (up to a rescaling of the coordinates). It easily follows from Ref. [46] that the duality holds in any dimension for our URL with $a = 1$ and a "Fermi-cube" point process, that is, a determinantal point process whose Fourier transform of the kernel is the indicator function of the unit cube (instead of sphere). The same duality does not hold for higher-order correlation functions.

The two-point function of the URL with $a = 1$ is perfectly cloaked, in the sense, that it is impossible to reconstruct the underlying long-range order from the pair correlation function alone. Higher-point correlation functions, however, can exhibit the periodicity of the original lattice. For cloaked URLs in $\mathbb{R}^d$ with $a = 1$, we have derived the n-point correlation functions of arbitrary order. In 1D, we explicitly demonstrate how g_4 reveals the periodicity of the underlying lattice in contrast to g_3, see Appendix D.

So an interesting open question for future research is how to construct isotropic amorphous hyperuniform point patterns or packings, for which samples with a million particles can easily be simulated (without any underlying lattice structure). For heterogeneous materials, the large-scale simulations of hyperuniform two-phase media that are fully amorphous have recently been made possible by a tessellation-based procedure [60], which locally enforces a global packing constraint in each cell.

APPENDIX A: DERIVATION OF THE STRUCTURE FACTOR OF THE PERTURBED LATTICE

Given a d-dimensional Bravais lattice $\mathcal{L}$, the points of the perturbed lattice can be represented by $x + u_x$, where $x \in \mathcal{L}$.

Here the displacements $\boldsymbol{u_x}$ are independent and identically distributed with a probability density function $f(\boldsymbol{u_x})$.

For a finite ball B_r with radius r (centered at the origin), we denote by n the number of points of $\mathcal{L}$ that fall into B_r. Then, we define the *scattering intensity* within the finite ball by

$$\mathcal{S}_{n,r}(\boldsymbol{k}) := \frac{1}{n}\mathbb{E}\left[\left|\sum_{\boldsymbol{x}\in\mathcal{L}\cap B_r}e^{-i\boldsymbol{k}\cdot(\boldsymbol{x}+\boldsymbol{u_x})}\right|^2\right], \quad \text{(A1)}$$

where $\mathbb{E}[\cdot]$ denotes an ensemble average.

In the thermodynamic limit, the structure factor $S(\boldsymbol{k})$ is then given by [61]

$$S(\boldsymbol{k}) := \lim_{r\to\infty}\mathbb{E}[\mathcal{S}_{n,r}(\boldsymbol{k})]. \quad \text{(A2)}$$

Using the mutual independence of the displacements, Eq. (A1) can be simplified to

$$\mathcal{S}_{n,r}(\boldsymbol{k}) = \frac{1}{n}\mathbb{E}\sum_{\boldsymbol{x},\boldsymbol{y}\in\mathcal{L}\cap B_r}e^{-i\boldsymbol{k}\cdot(\boldsymbol{x}-\boldsymbol{y})}e^{-i\boldsymbol{k}\cdot(\boldsymbol{u_x}-\boldsymbol{u_y})}$$

$$= 1 + |\underbrace{\mathbb{E}[e^{-i\boldsymbol{k}\cdot\boldsymbol{u}}]}_{=:\tilde{f}(\boldsymbol{k})}|^2\frac{1}{n}\mathbb{E}\sum_{\substack{\boldsymbol{x},\boldsymbol{y}\in\mathcal{L}\cap B_r\\\boldsymbol{x}\neq\boldsymbol{y}}}e^{-i\boldsymbol{k}\cdot(\boldsymbol{x}-\boldsymbol{y})},$$

where we denote by $\tilde{f}(\boldsymbol{k})$ the characteristic function, that is, the Fourier transformation of the probability density function f:

$$\tilde{f}(\boldsymbol{k}) := \mathcal{F}[f](\boldsymbol{k}) = \int_{\mathbb{R}^d}f(\boldsymbol{r})e^{-i\boldsymbol{k}\cdot\boldsymbol{r}}d\boldsymbol{r}. \quad \text{(A3)}$$

Note that $\tilde{f}(-\boldsymbol{k})$ is the complex conjugate of $\tilde{f}(\boldsymbol{k})$.

In the thermodynamic limit, the scattering intensity converges to Eq. (6):

$$S(\boldsymbol{k}) = 1 + |\tilde{f}(\boldsymbol{k})|^2(S_{\mathcal{L}}(\boldsymbol{k}) - 1), \quad \text{(A4)}$$

where $S_{\mathcal{L}}(\boldsymbol{k})$ is the structure factor of the lattice $\mathcal{L}$. In fact, the derivation is valid for more general point patterns.

APPENDIX B: PROOF OF THE NONSTEALTHY HYPERUNIFORMITY OF PERTURBED LATTICES

Stealthy hyperuniform point patterns are ones satisfying that $S(\boldsymbol{k}) = 0$ if $|\boldsymbol{k}| < K$ for some positive value of K [39]. We note that a perturbed lattice with independent and identically distributed displacements is stealthy hyperuniform if and only if the displacements are deterministic, that is, $f(\boldsymbol{u_x}) = \delta(\boldsymbol{u_x} - \boldsymbol{c})$ for some $\boldsymbol{c}\in\mathbb{R}^d$. This implies that perturbed lattices cannot be stealthy hyperuniform for any truly random perturbation.

From Eq. (6), the sufficient and necessary condition for a perturbed lattice to be stealthy hyperuniform is $|\tilde{f}(\boldsymbol{k})| = 1$ for all $|\boldsymbol{k}| < K$ for some positive value of K. Straightforwardly, any deterministic displacement meets this condition. We now show that only such deterministic shifts with vanishing variance fulfill this condition. We can show this for each coordinate separately because if the absolute value of the multivariate characteristic function is constant around the origin, then the same holds for each single coordinate.

Let U and V be two independent and identically distributed real-valued random variables with a characteristic function $\varphi(k)$ such that $|\varphi(k)|^2 = 1$ in a neighborhood around the

origin. We define the random variable $D := U - V$. Its characteristic function is given by $\varphi_D(k) := \varphi(k)\varphi^*(k) = |\varphi(k)|^2$. So it is by construction infinitely differentiable at the origin. Therefore, all moments of D exist, from which follows in turn that $\varphi_D(k)$ is an analytic function. Hence, $\varphi_D(k) = 1$ and $\mathbb{V}ar[D] = 0$. Since U and V are independent and identically distributed, $2\mathbb{V}ar[U] = \mathbb{V}ar[U - V] = \mathbb{V}ar[D] = 0$.

APPENDIX C: DERIVATION OF THE PAIR CORRELATION FUNCTION OF PERTURBED LATTICES

To obtain a stationary point pattern with a pair correlation function that does only depend on the relative position of two particles, we now consider a stationarized lattice. We shift the entire lattice $\mathcal{L}$ by a random vector that is uniformly distributed within a primitive unit cell. Then we perturb each point independently following the probability density function f. Note that this stationarized model has the same structure factor given by Eq. (6).

For a point pattern in the thermodynamic limit, its structure factor is directly related to its pair correlation function:

$$S(\boldsymbol{k}) = 1 + \rho\,\tilde{h}(\boldsymbol{k}),$$

where $\tilde{h}(\boldsymbol{k})$ is the Fourier transform of the total correlation function $h(\boldsymbol{r}) := g_2(\boldsymbol{r}) - 1$ and ρ is the number density.

Therefore, the pair correlation function of perturbed lattices with independent and identically distributed displacements is given by

$$g_2(\boldsymbol{r}) = 1 + \mathcal{F}^{-1}\left[\frac{S(\boldsymbol{k}) - 1}{\rho}\right](\boldsymbol{r})$$

$$= 1 + \frac{1}{\rho}\mathcal{F}^{-1}[\tilde{f}(\boldsymbol{k})\,\tilde{f}(-\boldsymbol{k})\,[S_{\mathcal{L}}(\boldsymbol{k}) - 1]](\boldsymbol{r}), \quad \text{(C1)}$$

where $\mathcal{F}^{-1}[\cdot](\boldsymbol{r})$ denotes the inverse Fourier transform. Note that the structure factor of a Bravais lattice $\mathcal{L}$ is

$$S_{\mathcal{L}}(\boldsymbol{k}) = (2\pi)^d\rho\sum_{\boldsymbol{q}\in\mathcal{L}^*\setminus\{\boldsymbol{0}\}}\delta(\boldsymbol{k} - \boldsymbol{q}), \quad \text{(C2)}$$

where $\mathcal{L}^*$ represents the reciprocal lattice of $\mathcal{L}$. Using Eq. (C2) and the convolution theorem, one can rewrite Eq. (C1) as

$$g_2(\boldsymbol{r}) = 1 - \frac{1}{\rho}\mathcal{F}^{-1}[\tilde{f}(\boldsymbol{k})\,\tilde{f}(-\boldsymbol{k})](\boldsymbol{r})$$

$$+ \sum_{\boldsymbol{q}\in\mathcal{L}^*\setminus\{\boldsymbol{0}\}}|\tilde{f}(\boldsymbol{q})|^2\cos(\boldsymbol{q}\cdot\boldsymbol{r})$$

$$= 1 - \frac{1}{\rho}f*f(\boldsymbol{r}) + \sum_{\boldsymbol{q}\in\mathcal{L}^*\setminus\{\boldsymbol{0}\}}|\tilde{f}(\boldsymbol{q})|^2\cos(\boldsymbol{q}\cdot\boldsymbol{r}),$$

where $f*g(\boldsymbol{r}) := \int_{\mathbb{R}^d}f(\boldsymbol{x})\,g(\boldsymbol{r} - \boldsymbol{x})\,d\boldsymbol{x}$ represents the convolution operation.

Evaluating the Fourier series with the Poisson summation formula, we obtain the pair correlation function of the perturbed lattice as

$$g_2(\boldsymbol{r}) = f*f*g_{\mathcal{L}}(\boldsymbol{r}) - \frac{1}{\rho}f*f(\boldsymbol{r}), \quad \text{(C3)}$$
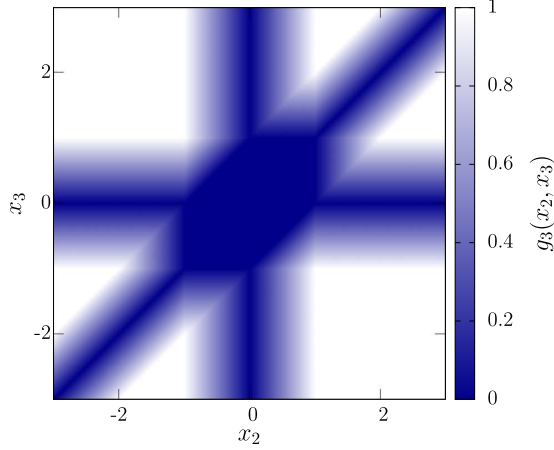
FIG. 8. Three-point correlation function $g_3(0, x_2, x_3)$ of the 1D cloaked URL with $a = 1$. The long-range order of the original lattice remains cloaked at the three-point level, in the sense that there are no features that exhibit the periodicity of the underlying lattice.

where

$$g_{\mathcal{L}}(\mathbf{r}) = \frac{1}{\rho} \sum_{\mathbf{x} \in \mathcal{L}} \delta(\mathbf{r} - \mathbf{x}). \tag{C4}$$

Inserting Eq. (C4) into Eq. (C3), we obtain Eq. (7), which can also be written as:

$$g_2(\mathbf{r}) = \frac{1}{\rho} \sum_{\mathbf{x} \in \mathcal{L} \setminus \{\mathbf{0}\}} f * f(\mathbf{r} - \mathbf{x}). \tag{C5}$$

For the URL in d-dimensional Euclidean space, the probability density functions of different coordinates are independent of each other. So the convolution in Eq. (C5) factorizes:

$$f * f(\mathbf{r}) = \frac{1}{a^d} \prod_{i=1}^{d} \left(1 - \frac{|x_i|}{a}\right) \mathbf{1}_{[-a,a]}(x_i), \tag{C6}$$

where $\mathbf{r} = (x_1, x_2, \dots)$.

In the case of cloaking, i.e., $a \in \mathbb{N} \setminus \{\mathbf{0}\}$, the total correlation function $h(\mathbf{r})$ also factorizes:

$$h(\mathbf{r}) := \frac{-1}{a^d} \prod_{i=1}^{d} \left(1 - \frac{|x_i|}{a}\right) \mathbf{1}_{[-a,a]}(x_i). \tag{C7}$$

APPENDIX D: DERIVATION OF THE n-POINT CORRELATION FUNCTIONS OF CLOAKED URLS

For URLs with $a = 1$, we derive here the n-point correlation functions in arbitrary dimension d. First, we state the n-point correlation function $g_n^{(0)}(\mathbf{x}_1, \dots \mathbf{x}_n)$ for a statistically inhomogeneous model that uses a fixed lattice $\mathcal{L}$. Since each lattice point $\mathbf{y}_i \in \mathcal{L}$ is uniformly distributed within its unit cell
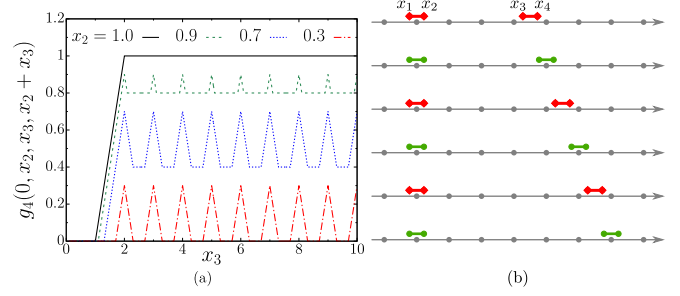

FIG. 9. Four-point correlation function $g_4(0, x_2, x_3, x_4)$ of the 1D cloaked URL with $a = 1$ (a) as a function of x_3 choosing a specific path in configuration space, where x_1 and x_2 are constant and $x_4 = x_2 + x_3$. The curves represent four different values of x_2 (assuming without loss of generality that $x_1 = 0$). In contrast to the two-point and three-point correlation functions, the periodicity of the original lattice can be identified for $0 < x_2 < 1$. (b) The schematic explains the occurrence of this periodicity. The gray dots represent the unit cell boundaries of the original lattice. There cannot be two particles within a single unit cell of the lattice. Therefore, the contribution of cases 1, 3, and 5 [counted from top to bottom, colored red (diamonds)] to g_4 is identically zero.

$C + \mathbf{y}_i$, $g_n^{(0)}$ is 0 if a pair of distinct points $\mathbf{x}_i$ and $\mathbf{x}_j$ in the same unit cell or 1 otherwise.

For a statistically homogeneous URL [62], the n-point correlation function is given by

$$g_n(\mathbf{x}_1, \dots \mathbf{x}_n) = \frac{1}{|C|} \int_C g_n^{(0)}(\mathbf{x}_1 - \mathbf{u}, \dots \mathbf{x}_n - \mathbf{u}) d\mathbf{u}$$

$$= 1 - \frac{1}{|C|} \left| \bigcup_{\substack{i,j=1,\dots n \\ i \neq j}} S(\mathbf{x}_i, \mathbf{x}_j) \right|,$$

where $S(\mathbf{x}_i, \mathbf{x}_j)$ denotes the set of all points $\mathbf{u} \in C$, for which $\mathbf{x}_i - \mathbf{u}$ and $\mathbf{x}_j - \mathbf{u}$ are in the same unit cell. Thus, the last term represents the probability for finding at least one pair of points inside the same unit cell if all points are shifted by the same vector $\mathbf{u}$ uniformly distributed on C. Without loss of generality, we assume that $C = -C$. To prove Eq. (9), it remains to be shown that $S(\mathbf{x}_i, \mathbf{x}_j) = C_{ij}^*$.

Assume that $\mathbf{u} \in S(\mathbf{x}_i, \mathbf{x}_j)$. Then there exists $\mathbf{l} \in \mathcal{L}$ so that $\mathbf{x}_i - \mathbf{u} \in C + \mathbf{l}$ and $\mathbf{x}_j - \mathbf{u} \in C + \mathbf{l}$. Therefore $(-\mathbf{u}) \in (C - \mathbf{x}_i) \cap (C - \mathbf{x}_j) + \mathbf{l}$. Using $C = -C$, $(-\mathbf{l}) \in \mathcal{L}$, and $S(\mathbf{x}_i, \mathbf{x}_j) \subset C$, it follows that $\mathbf{u} \in C_{ij}^*$, and thus $S(\mathbf{x}_i, \mathbf{x}_j) \subset C_{ij}^*$.

Assume that $\mathbf{u} \in C_{ij}^*$. Then there exists $\mathbf{l} \in \mathcal{L}$ so that $\mathbf{u} \in (C + \mathbf{x}_i) \cap (C + \mathbf{x}_j) + \mathbf{l}$ and therefore $\mathbf{x}_i - \mathbf{u} \in C - \mathbf{l}$ and $\mathbf{x}_j - \mathbf{u} \in C - \mathbf{l}$. Hence, $\mathbf{u} \in S(\mathbf{x}_i, \mathbf{x}_j)$, and thus $C_{ij}^* \subset S(\mathbf{x}_i, \mathbf{x}_j)$.

For the cloaked URL in 1D, Fig. 8 displays the three-point correlation function. It has no features with the periodicity of the underlying lattice. However, this periodicity can be extracted from the four-point function shown in Fig. 9.

[1] T. R. Welberry, G. H. Miller, and C. E. Carroll, Acta Crystallogr. A **36**, 921 (1980).

[2] W. J. Stroud and R. P. Millane, Proc. R. Soc. Lond. A **452**, 151 (1996).

[3] C. Helgert, C. Rockstuhl, C. Etrich, E.-B. Kley, A. Tünnermann, F. Lederer, and T. Pertsch, Appl. Phys. A **103**, 591 (2011).

[4] M. Albooyeh, S. Kruk, C. Menzel, C. Helgert, M. Kroll, A. Krysinski, M. Decker, D. N. Neshev, T. Pertsch, C. Etrich, C. Rockstuhl, S. A. Tretyakov, C. R. Simovski, and Y. S. Kivshar, Sci. Rep. **4**, 4484 (2014).

[5] This extends to any periodic point pattern with high crystallographic symmetries.

[6] A. Gabrielli, Phys. Rev. E **70**, 066131 (2004).

[7] S. Ghosh and J. L. Lebowitz, Ind. J. Pure Appl. Math. **48**, 609 (2017).

[8] J. Kim and S. Torquato, Phys. Rev. B **97**, 054105 (2018).

[9] A. Gabrielli, M. Joyce, and F. S. Labini, Phys. Rev. D **65**, 083523 (2002).

[10] T. Baertschiger, M. Joyce, A. Gabrielli, and F. S. Labini, Phys. Rev. E **75**, 021113 (2007).

[11] M. Sodin and B. Tsirelson, Israel J. Math. **152**, 105 (2006).

[12] Y. Peres and A. Sly, arXiv:1409.4490 (2014).

[13] S. Ghosh and J. Lebowitz, J. Stat. Phys. **166**, 1016 (2016).

[14] M. A. Klatt, G. Last, and D. Yogeshwaran, arXiv:1810.00265 (2018).

[15] S. Asmussen, *Applied Probability and Queues*, 2nd ed., Applications of Mathematics No. 51 (Springer, New York, 2003).

[16] S. Goldstein, J. L. Lebowitz, and E. R. Speer, Markov Processes Relat. Fields **12**, 235 (2006).

[17] G. Efstathiou, M. Davis, S. D. M. White, and C. S. Frenk, Astrophys. J., Suppl. Ser. **57**, 241 (1985).

[18] E. Renshaw, Biom. J. **44**, 718 (2002).

[19] S. Torquato and F. H. Stillinger, Phys. Rev. E **68**, 041113 (2003).

[20] A. T. Chieco, R. Dreyfus, and D. J. Durian, Phys. Rev. E **96**, 032909 (2017).

[21] Simple examples of Bravais lattices are the triangular and square lattice in 2D and the face-centered, body-centered, and simple cubic lattices in 3D.

[22] K. Aydin, K. Guven, N. Katsarakis, C. M. Soukoulis, and E. Ozbay, Opt. Express **12**, 5896 (2004).

[23] C. Helgert, C. Rockstuhl, C. Etrich, C. Menzel, E.-B. Kley, A. Tünnermann, F. Lederer, and T. Pertsch, Phys. Rev. B **79**, 233107 (2009).

[24] N. Papasimakis, V. A. Fedotov, Y. H. Fu, D. P. Tsai, and N. I. Zheludev, Phys. Rev. B **80**, 041102(R) (2009).

[25] R. Singh, X. Lu, J. Gu, Z. Tian, and W. Zhang, J. Opt. **12**, 015101 (2009).

[26] C. Rockstuhl, C. Menzel, S. Mühlig, J. Petschulat, C. Helgert, C. Etrich, A. Chipouline, T. Pertsch, and F. Lederer, Phys. Rev. B **83**, 245119 (2011).

[27] D. Mogilevtsev and A. Maloshtan, Phys. Rev. B **84**, 113105 (2011).

[28] M. Albooyeh, D. Morits, and S. A. Tretyakov, Phys. Rev. B **85**, 205110 (2012).

[29] Z. Awan and A. Rizvi, Opt. Commun. **309**, 338 (2013).

[30] S. Yu, X. Piao, J. Hong, and N. Park, Sci. Adv. **2**, e1501851 (2016).

[31] S. Torquato, Phys. Rep. **745**, 1 (2018).

[32] E. C. Oğuz, J. E. S. Socolar, P. J. Steinhardt, and S. Torquato, Phys. Rev. B **95**, 054119 (2017).

[33] D. Hexner and D. Levine, Phys. Rev. Lett. **118**, 020601 (2017).

[34] Q.-L. Lei and R. Ni, Proc. Natl. Acad. Sci. U.S.A. **116**, 22983 (2019).

[35] D. Levesque, J.-J. Weis, and J. Lebowitz, J. Stat. Phys. **100**, 209 (2000).

[36] B. Jancovici, Phys. Rev. Lett. **46**, 386 (1981).

[37] J. Ginibre, J. Math. Phys. **6**, 440 (1965).

[38] C. E. Zachary and S. Torquato, J. Stat. Mech. Theory Exp. (2009) P12015.

[39] S. Torquato, G. Zhang, and F. H. Stillinger, Phys. Rev. X **5**, 021020 (2015).

[40] G. Zhang, F. H. Stillinger, and S. Torquato, Sci. Rep. **6**, 36963 (2016).

[41] M. Florescu, S. Torquato, and P. J. Steinhardt, Proc. Natl. Acad. Sci. U.S.A. **106**, 20658 (2009).

[42] M. Castro-Lopez, M. Gaio, S. Sellers, G. Gkantzounis, M. Florescu, and R. Sapienza, APL Photon. **2**, 061302 (2017).

[43] S. Gorsky, W. A. Britton, Y. Chen, J. Montaner, A. Lenef, M. Raukas, and L. Dal Negro, APL Photon. **4**, 110801 (2019).

[44] O. Leseur, R. Pierrat, and R. Carminati, Optica **3**, 763 (2016).

[45] R. P. Feynman and M. Cohen, Phys. Rev. **102**, 1189 (1956).

[46] S. Torquato, A. Scardicchio, and C. E. Zachary, J. Stat. Mech. Theory Exp. (2008) P11019.

[47] A. Donev, F. H. Stillinger, and S. Torquato, Phys. Rev. Lett. **95**, 090604 (2005).

[48] Y. Jiao and S. Torquato, Phys. Rev. E **84**, 041309 (2011).

[49] C. E. Zachary and S. Torquato, Phys. Rev. E **83**, 051133 (2011).

[50] D. Hexner and D. Levine, Phys. Rev. Lett. **114**, 110602 (2015); Z. Ma and S. Torquato, Phys. Rev. E. **99**, 022115 (2019).

[51] D. S. Novikov, J. H. Jensen, J. A. Helpern, and E. Fieremans, Proc. Natl. Acad. Sci. U.S.A. **111**, 5088 (2014).

[52] Q. Le Thien, D. McDermott, C. J. O. Reichhardt, and C. Reichhardt, Phys. Rev. B **96**, 094516 (2017).

[53] Here, cloaking refers to this vanishing of Bragg peaks and not to a complete invisibility of the system.

[54] A. Gabrielli and S. Torquato, Phys. Rev. E **70**, 041105 (2004). References [6] and [54] contained only brief side remarks about the complete cancellation of the Bragg peak contribution being only possible for a very peculiar case fixing the zeros of the characteristic function of perturbations.

[55] S. Torquato, G. Zhang, and M. D. Courcy-Ireland, J. Phys. A: Math. Theor. **52**, 135002 (2019).

[56] For a single configuration with N points at positions $r_1, r_2, \ldots$ under periodic boundary conditions, the structure factor including the forward scattering peak at the origin is equivalent to the scattering intensity $\mathcal{S}(\boldsymbol{k}) := \| \sum_{j=1}^{N} e^{-i\boldsymbol{k}\cdot\boldsymbol{r}_j} \|^2/N$, where $\boldsymbol{k}$ is a reciprocal lattice vector of the periodic simulation box.

[57] The constant can easily be obtained from Eq. (11) by substituting $\boldsymbol{k}$ by $\boldsymbol{x}/a$: $c := \frac{1}{\pi D} \int_{\mathbb{R}^d} [1 - \prod_{i=1}^{d} \sin^2(x_i/2)/(x_i/2)^2] / \|\boldsymbol{x}\|^{d+1} d\boldsymbol{x}$.

[58] It uses $\sin^2(x) < 1$ for all $x \in \mathbb{R}$.

[59] S. Atkinson, F. H. Stillinger, and S. Torquato, Phys. Rev. E **94**, 032902 (2016).

[60] J. Kim and S. Torquato, Acta Mater. **168**, 143 (2019).

[61] J.-P. Hansen and I. R. McDonald, *Theory of Simple Liquids: With Applications to Soft Matter*, 4th ed. (Academic Press, Boston, 2013).

[62] The statistically homogeneous URL is based on a stationarized lattice $\mathcal{L} + U$, where the random vector U is uniformly distributed on the unit cell C.